Contents lists available at ScienceDirect

Arabian Journal of Chemistry

journal homepage: www.ksu.edu.sa

# NMR-based metabolomics and UHPLC-ESI-MS/MS profiling of *Syzygium jambos* in relation to their antioxidant and anti-hyperglycemic activities

Pei Lou WONG [a], Nurul Shazini RAMLI [a], Chin Ping TAN [b], Azrina AZLAN [c], Faridah ABAS [a,d,*]

[a] Department of Food Science, Faculty of Food Science and Technology, Universiti Putra Malaysia, 43400, Serdang, Selangor, Malaysia
[b] Department of Food Technology, Faculty of Food Science and Technology, Universiti Putra Malaysia, 43400, Serdang, Selangor, Malaysia
[c] Department of Nutrition and Dietetics, Faculty of Medicine and Health Sciences, Universiti Putra Malaysia, Serdang, Selangor, Malaysia
[d] Natural Medicines and Products Research Laboratory, Institute of Bioscience, Universiti Putra Malaysia, 43400, Serdang, Selangor, Malaysia

ARTICLE INFO

*Keywords:*
*Syzygium jambos*
$^{1}$H NMR metabolomics
Antioxidant
Anti-hyperglycemic
UHPLC-ESI-MS/MS metabolites profiling

ABSTRACT

Search for natural sources in disease management especially diabetes has surged recently for its potential health benefits. However, several fruit tree species remained unpopular despite their folkloric usage due to insufficient scientific data. *Syzygium jambos* (L.) Alston (Myrtaceae) is a fruit-bearing plant that is used as a traditional dietary supplement to treat various diseases including diabetes. This study investigated the correlation between *S. jambos* leaves' metabolites and the bioactivities using proton-nuclear magnetic resonance ($^{1}$H NMR)-based metabolomics approach. *In-vitro* total phenolic content (TPC), 2,2-diphenyl-1-picrylhydrazyl (DPPH•) radicals scavenging, nitric oxide (NO•) radicals scavenging, anti-α-amylase and anti-α-glucosidase assays were performed. The findings indicated that 70 % ethanolic extract demonstrated the highest potential in overall bioactivities. A total of 59 and 30 metabolites were tentatively identified using ultrahigh-performance liquid chromatography electrospray ionization Quadrupole-Orbitrap tandem mass spectrometry (UHPLC/ESI Q-Orbitrap MS/MS) and NMR, respectively. The partial least square (PLS) model revealed tannins, triterpenoids, and flavonoids significantly contributed to the separation and bioactivities. This study provides comprehensive insights into *S. jambos* metabolome and reveals the potential as a reliable source of antioxidant and anti-hyperglycemic compounds.

## 1. Introduction

Diabetes has appeared as one of the most common chronic diseases with life-threatening complications and reduction of life expectancy. According to International Diabetes Federation (IDF), the global prevalence of diabetes in adults aged 20–79 years old is estimated to rocket to 12.2 % in 2045 from 10.5 % in 2021 (Sun et al., 2022). Generally, type 2 diabetes mellitus (T2DM) accounted for most of the diabetes events which are characterized by its ineffective utilization of insulin and progressive insulin resistance. Over decades, hyperglycemia and impaired glucose tolerance in T2DM have been effectively controlled in several medical approaches including insulin and oral hypoglycemic drugs as antioxidant agents and carbohydrate hydrolyzing enzyme inhibitors (WHO, 2016). One of the strategic approaches in diabetes treatment is to mitigate postprandial hyperglycemia by delaying and reducing glucose absorption, which responsible for starch hydrolyzing enzymes, α-amylase and α-glucosidase (Alqahtani et al., 2020). In recent years, herbal therapy has been a leading field in managing diabetes together with conventional treatment procedures to enhance patients' wellness and health systems. Therefore, scientific investigation is essential to reveal the natural therapeutic characteristics and to support the traditional claims of medicinal plants.

*Abbreviations:* AA, anti-α-amylase; AG, anti-α-glucosidase; CID, collision-induced dissociation; DNS, 3,5-Dinitrosalicylic acid; DPPH•, 2,2-diphenyl-1-picrylhydrazyl; FA, formic acid; HHDP, hexahydroxydiphenoyl; HMBC, heteronuclear multiple bond correlation; HSQC, heteronuclear single quantum coherence; IDF, International Diabetes Federation; MS, mass spectrometry; NMR, nuclear magnetic resonance; NO•, nitric oxide; PCA, principal component analysis; PLS, partial least square; PNPG, *p*-nitrophenyl-α-D-glucopyranose; SNP, sodium nitroprusside; T2DM, type 2 diabetes mellitus; TOCSY, total correlation spectroscopy; TPC, total phenolic content; UHPLC-ESI-MS, ultrahigh-performance liquid chromatography-electrospray ionization-mass spectrometry; VIP, variable importance in the projection.

Peer review under responsibility of King Saud University.

* Corresponding author.
*E-mail addresses:* gs53905@student.upm.edu.my (P.L. WONG), shazini@upm.edu.my (N.S. RAMLI), tancp@upm.edu.my (C.P. TAN), azrinaaz@upm.edu.my (A. AZLAN), faridah_abas@upm.edu.my (F. ABAS).

https://doi.org/10.1016/j.arabjc.2023.105546
Received 23 August 2023; Accepted 7 December 2023
Available online 9 December 2023

*Syzygium jambos* (L.) Alston (Myrtaceae), is a medium-sized fruit tree commonly known as rose apple or "jambu mawar" in Malaysia and is found to be native to Southeast Asia and cultivated in other warm tropical regions, such as East India and South America (Baliga et al., 2017). *S. jambos* has a history of being extensively used as herb and for folk medicine. A decoction of the leaves could be used as diuretic for treating rheumatism, inflammatory pain, and diabetes. Moreover, ingestion of the juice of macerated leaves can help alleviate fever, sore throat, and sore eyes, and powdered leaves applied topically can act as a cooling agent for patients with smallpox (Avila-Pena et al., 2007; Bonfanti et al., 2013; Morton, 1987). Other plant parts, such as fruit, flower, seed, and bark, can also be used as various traditional remedies for diarrhea, dysentery, asthma, bronchitis, and dysphonia (Morton, 1987). *S. jambos* was reported to exhibit antinociceptive, analgesic (Avila-Pena et al., 2007), anti-microbial, anti-inflammatory (Sharma et al., 2013), anti-cancer (Yang et al., 2000), and hepato-protective (Islam et al., 2012) properties. Phytochemical studies on *S. jambos* leaves have identified several secondary metabolites, including flavonoids (catechin, rutin, quercetin, and ellagic acid) (Hossain et al., 2016), hydrolyzable tannins (pedunculagin, casuarinin, and castalagin) (Yang et al., 2000), and dihydrochalcones (myrigalone derivatives and phloretin) (Jayasinghe et al., 2007).

In view of the reported anti-hyperglycemic effect of *S. jambos* (Gavillán-suárez et al., 2015), an investigation into the possibility of additive effects among plant bioactive compounds and its pharmacological implications is warranted. Metabolomics provides a thorough phytochemical profile rather than an individual compound analysis, which reveals the variation of phytoconstituents in different environments and the corresponding interactions (Wolfender et al., 2013). The common techniques used in metabolomics studies are nuclear magnetic resonance (NMR) and mass spectrometry (MS). Proton NMR ($^1$H NMR) is a robust instrument for the metabolites analysis qualitatively and quantitatively in a matrix, whereas two-dimensional NMR (2D-NMR) is usually employed to increase resolution, particularly in overlapping signals (Wolfender et al., 2013). NMR is widely used coupled with multivariate data analysis in phytochemical studies (Kim et al., 2011).

In the search for solvent efficiency in the extraction of bioactive metabolites from the *S. jambos* leaves, this study aimed to investigate the metabolite difference in *S. jambos* leaves extracted with four ethanol/water ratios using the NMR-based metabolomics technique. This allows the annotation of phytochemicals and the correlation between the antioxidant and anti-hyperglycemic properties of the plant. Moreover, the present study provides a thorough metabolite profile of the *S. jambos* leaf extract using ultrahigh-performance liquid chromatography electrospray ionization (UHPLC/ESI) Orbitrap MS. Hence, this study provides a comprehensive profile for the distribution of the bioactive compounds in *S. jambos* leaves extracts as a reliable source of functional foods which further proves its traditional usage in diabetes management.

## 2. Materials and methods

### 2.1. Chemicals and reagents

Deuterated methanol-$d_4$ ($CD_3OD$), deuterium oxide ($D_2O$), non-deuterated potassium dihydrogen phosphate ($KH_4PO_4$), sodium deuterium oxide (NaOD), Folin–Ciocalteu reagent, trimethylsilylpropionic acid-d4 sodium salt (TSP) and absolute ethanol were obtained from Merck (Darmstadt, Germany). 2,2-diphenyl-1-picrylhydrazyl (DPPH•), sodium carbonate, sodium nitroprusside (SNP), α-amylase enzyme, α-glucosidase enzyme, glycine, phosphate buffered saline, *p*-nitrophenyl-α-D-glucopyranose (PNPG), sodium chloride (NaCl), 3,5-Dinitrosalicylic acid (DNS), sodium potassium tartrate tetrahydrate, potato starch, quercetin, gallic acid and acarbose were supplied by Sigma-Aldrich Co. (St Louis, MO, USA). Dimethyl sulfoxide (DMSO), LCMS-grade methanol, LCMS-grade water and formic acid (FA) were obtained from Fisher Scientific (Geel, Belgium).

### 2.2. Plant collection and extraction

*Syzygium jambos* (voucher number MFI 0053/19) was collected from Universiti Putra Malaysia (UPM), Malaysia, identified and deposited by an in-house botanist from Biodiversity Unit, Dr. Mohd Firdaus Ismail at Institute of Bioscience, UPM. The leaves were collected from six trees to serve as biological replications. The cleaned leaves were air-dried at room temperature (23–26 °C) before being pulverized into powder using a laboratory pulverizer (Waring Commercial, Torrington, CT, USA) (Mediani et al., 2014). The extraction process was performed by adding 10 g of plant sample into 100 mL of four different ethanol/water ratios (0 %, 50 %, 70 %, and absolute ethanol) then subjected to ultrasonication for 1 h (53 kHz) under temperature 26–40 °C using a Thermo-10D Ultrasonic machine (Fisher Scientific, Waltham, MA, USA). The crude extracts were then filtered, and vacuum concentrated at 40 °C. The extraction procedure was conducted twice using the same filtration residue. All the weighed crude extracts were subjected to freeze-dry using ScanVac CoolSafe Freeze dryer (Labogene, Lynge, Denmark), and kept at 4 °C for future analysis.

### 2.3. Total phenolic content (TPC) assay

TPC was determined by Folin–Ciocalteu (FC) procedure with slight amendments (Zhang et al., 2006). 100 μL of FC reagent was mixed with 20 μL of 100 μg/mL sample in a 96-well plate. The sample was prepared by dissolution of freeze-dried crude extract with 10 % DMSO for *in-vitro* biological assays. After 5 min incubation, 80 μL of 7.5 % sodium carbonate was added to the well, and the mixture was then incubated in the dark for 30 min. Then, the absorbance was detected at 750 nm using Tecan Infinite F200 micro-plate reader (Tecan Group Ltd, Männedorf, Switzerland). Gallic acid was used to obtain the calibration curve. The results obtained were then expressed in mg of gallic acid equivalent per crude extract of *S. jambos* (mg GAE/g).

### 2.4. DPPH• free radicals scavenging assay

The DPPH• assay was performed using the described method (Wan et al., 2012) with slight modifications. 100 μL of DPPH• reagent was added into 50 μL of the serial diluted sample. The absorbance was then detected at 515 nm after 30 min of incubation in the dark at room temperature. The scavenging capacity (SC) was calculated as $SC\% = [(A_0 - A_s)/A_0] \times 100$, where $A_0$ is the absorbance of reagent blank, while $A_s$ is the absorbance of test sample. The results were expressed in half maximal inhibitory concentration ($IC_{50}$), and quercetin was served as a positive control.

### 2.5. Nitric oxide (NO•) radicals scavenging assay

NO• radical scavenging assay was performed by mixing 60 μL of 10 mM SNP into 60 μL of the serial diluted plant sample and incubated for 150 min at room temperature. 60 μL of Griess reagent (freshly prepared) was then added to the mixture before the absorbance was detected at 550 nm. The obtained results were expressed in $IC_{50}$, gallic acid and quercetin served as a positive control (Tsai et al., 2007).

### 2.6. Anti-α-amylase (AA) assay

The anti-α-amylase assay was evaluated using the method with relevant adjustments (Telagari & Hullatti, 2015). The enzymatic reaction was achieved using 1 % potato starch solution as substrate and α-amylase enzyme, both prepared in 100 mM sodium phosphate buffer (pH 6.9). A mixture of 10 μL serial diluted test samples and 50 μL of 100 mM buffer was mixed with 10 μL of α-amylase enzyme (2U/mL) in 96-well plate. The blank solvent and blank sample were comprised of 60

μL of 100 mM sodium phosphate buffer and 10 μL of solvent, and 60 μL of 100 mM sodium phosphate buffer and 10 μL of test sample, respectively. Negative control was assembled by replacing the test sample with solvent, and the mixture was then incubated for 20 min at 37 °C. After that, 20 μL of 1 % starch solution was mixed into the wells of test sample, positive and negative controls, whereas the rest was added with 20 μL of 100 mM sodium phosphate buffer. A volume of 100 μL DNS reagent was then added into the mixture to quench the reaction after incubation at 37 °C for 30 min. Then, the mixture was brought to 90 °C for 10 min before the absorbance reading was measured at 550 nm. The percentage of inhibition was determined as %Inhibition = $[(a_n - a_s)/a_n]$ x 100, where $a_n$ is the absorbance difference between blank and negative control, and $a_s$ is the absorbance difference between a sample and blank sample. Positive control used in this assay was acarbose and the results were expressed in $IC_{50}$.

### 2.7. Anti-α-glucosidase (AG) assay

This experiment was performed by the method described (Lee et al., 2019). The enzymatic reaction was accomplished using PNPG (substrate) and α-glucosidase (enzyme). A mixture of 10 μL serial diluted test samples and 130 μL of 30 mM phosphate buffer was mixed with 10 μL of α-glucosidase enzyme in a 96-well plate. The blank sample, blank solvent and negative control were prepared accordingly, and the mixture was then incubated for 5 min at room temperature. After that, 50 μL of PNPG was mixed with test sample, positive and negative controls, while the rest was added with 50 μL of 30 mM sodium phosphate buffer. A volume of 50 μL 2 M glycine (pH 10) was added into the mixture to cease the reaction after incubation for 15 min. The absorbance reading was detected at 405 nm, and the percentage of inhibition was determined similarly to the anti-α-amylase assay. Positive control used in this assay was quercetin and acarbose, and the results obtained were expressed in $IC_{50}$.

### 2.8. $^1$H NMR analysis and spectra processing

The experiment of $^1$H NMR was conducted based on the method described (Abdul-Hamid et al., 2019). Generally, 10 mg of test sample was dissolved in 375 μL of $CD_3OD$ and 375 μL of $KH_2PO_4$ buffer in $D_2O$ containing 0.1 % TSP (pH 6.0). The mixture was sonicated for 15 min and centrifuged for 10 min at 13000 rpm. The supernatant was then subjected to $^1$H NMR analysis using a Varian INOVA 500 MHz NMR spectrometer (Varian Inc., Palo Alto, CA, USA). The PRESAT was employed to suppress the broad water signal. The acquisition time is 4.29 min with 64 scans, spectral width and relaxation delay were reported as 16 ppm, 2.045 s, 8.6 ms, and 2.0 s, respectively. 2D-NMR experiments were performed. *J-res* spectrum was measured through 8 K for the chemical shift axis and spectral width of 66 Hz with a relaxation delay of 1.5 s, 8 scans per 256 increments, and spectral width of 5000 Hz for the axis of the spin–spin coupling constant. TOCSY spectrum was performed with 16 scans per 256 increments, and 1.0 s relaxation delay in 2 h and 54 min total experiment run time, while HSQC and HMBC spectra were obtained by 32 scans per 256 increments, with relaxation delays of 1.0 s, in a total experiment run time of 5 h and 33 min, and 5 h and 43 min, respectively. All the processed spectra were binned using Chenomx software (Edmonton, AB, Canada). All spectra were binned and exported into Excel file for MVDA which were performed on the binned integrals of the $^1$H NMR data using SIMCA-P + software version 14.1 (Umetrics, Umeå, Sweden). Principal component analysis (PCA) and partial least squares (PLS) models were generated using the Pareto scaling method (Pramai et al., 2018).

### 2.9. UHPLC-MS/MS analysis

The measurement was conducted using method described (Wong et al., 2020). The UHPLC-MS/MS spectra in negative ion mode were acquired from 150 to 1500 *m/z* with collision-induced dissociation (CID) energy of 30 % using Thermo Scientific™ Q Exactive™ Hybrid Quadrupole-Orbitrap mass spectrometer equipped with autosampler and surveyor UHPLC binary pump coupled with electrospray ionization (ESI) source (Thermo Fisher Scientific, Bremen, Germany). The mobile phase used was LCMS-grade water (solvent A) and acetonitrile (solvent B) with each consisting of 0.1 % FA. The programmed gradient was commenced with 95 % to 0 % solvent A from 0.5 to 30 min at a flow rate of 0.4 mL/min. The phytochemical separation was determined by an Acquity UPLC HSS T3 column (1.8 μm, 2.1 x 100 mm), with a 2 μL injection volume of 10 mg/mL sample. The obtained spectra were processed and analyzed using Thermo Xcalibur Qual Browser software 4.0 (Thermo Fisher Scientific Inc., Waltham, MA, USA). The peak identification was accomplished by comparison of deprotonated molecular ion and fragmentation patterns with mass tolerance at 0.01 Da (Olsen et al., 2005).

### 2.10. Statistical analysis

The results of biological activities were displayed as the mean ± standard deviation of six biological replicates. The significant difference of factors between groups at 95 % confidence level was determined using One-way ANOVA with Tukey's post hoc test. Statistical analysis was accomplished by using IBM SPSS Statistics 20 (SPSS Inc., Chicago, IL, USA) and MS Excel 2013 (Microsoft, Redmond, WA, USA).

## 3. Results

### 3.1. Effects of extraction solvent ratio on biological activities

The impacts of solvent systems on the TPC and biological activities of *S. jambos* leaves are presented in Table 1. The use of 50 % and 70 % ethanol was able to extract higher yield from *S. jambos* leaves compared with the use of water and absolute ethanol extracts. The absolute ethanol extract retained the highest TPC without statistical difference with 70 % ethanolic extract followed by 50 % ethanolic and water extract. In antioxidant activities, the results (Table 1) indicated that the $IC_{50}$ values of the DPPH• activity ranged from 2.49 ± 0.26 to 7.72 ± 0.42 μg/mL. The water extract (0 %) showed the highest DPPH• radical scavenging capacity without significant difference with 70 % ethanolic extract. Meanwhile, all the $IC_{50}$ values of the extracts were higher than those of gallic acid and quercetin in the NO• assays (15.41 ± 0.63 and 15.85 ± 0.58 μg/mL, respectively). The water, absolute ethanol, and 70 % ethanolic extracts exhibited $IC_{50}$ values close to 42 μg/mL without significant difference.

The results (Table 1) indicated that the 70 % ethanolic extract demonstrated the most active in both anti-α-amylase and anti-α-glucosidase assays with $IC_{50}$ values of 83.43 ± 3.40 μg/mL and 0.52 ± 0.01 μg/mL, respectively. In contrast, the water extract showed the lowest activity in both the α-amylase and α-glucosidase enzyme inhibition, with $IC_{50}$ values of 752.97 ± 103.66 μg/mL and 30.41 ± 4.23 μg/mL, respectively.

### 3.2. Metabolite identification via NMR

The presence of metabolites in *S. jambos* leaves extracted at different ethanol/water ratios was investigated using a combination of the 1D $^1$H NMR and 2D-NMR (*J*-res, TOCSY, HSQC and HMBC) techniques. Fig. S1 presents the representative $^1$H NMR spectra of *S. jambos* leaves of different extracts. *J*-res analysis (Fig. S2) was conducted to elucidate the overlapping signals and to determine the coupling constants, TOCSY (Fig. S3) explained the correlations of protons within a spin system, whereas HSQC and HMBC (Fig. S4 and S5) provide proton-carbon single bond and multiple bonds correlations (Abdul-Hamid et al., 2019). The tentative metabolite identification was based on literature data comparison and quest for several available online databases (Chenomx

**Table 1**
Yield of extraction, TPC, DPPH• and NO• radicals scavenging, anti-α-amylase and anti-α-glucosidase assays of *S. jambos* leaves extracted with 0%, 50%, 70% and absolute ethanol.

| Solvent system | Yield of extraction (%) | TPC (mg GAE / g crude extract) | DPPH• scavenging assay $IC_{50}$ (μg/mL) | NO• scavenging assay $IC_{50}$ (μg/mL) | Anti-α-amylase assay $IC_{50}$ (μg/mL) | Anti-α-glucosidase assay $IC_{50}$ (μg/mL) |
|---|---|---|---|---|---|---|
| 0 % | 21.26 ± 1.34 [b] | 323.23 ± 20.46 [b] | 2.49 ± 0.26 [a] | 42.72 ± 3.51[b] | 752.97 ± 103.66 [c] | 30.41 ± 4.23 [e] |
| 50 % | 24.91 ± 1.35 [a] | 324.78 ± 19.17 [b] | 3.18 ± 0.25 [b] | 53.62 ± 2.79 [c] | 88.40 ± 5.36 [b] | 5.62 ± 0.69 [c] |
| 70 % | 24.89 ± 0.98 [a] | 386.37 ± 36.48 [a] | 2.73 ± 0.07 [a] | 42.08 ± 3.76 [b] | 83.43 ± 3.40 [b] | 0.52 ± 0.01 [a] |
| Abs | 14.05 ± 1.44 [c] | 425.04 ± 42.19 [a] | 7.72 ± 0.42 [c] | 42.34 ± 3.62 [b] | 89.51 ± 6.75 [b] | 0.90 ± 0.07 [b] |
| Quercetin | – | – | 3.55 ± 0.28 [b] | 15.85 ± 0.58 [a] | – | 6.62 ± 0.03 [c] |
| Gallic acid | – | – | – | 15.41 ± 0.63 [a] | – | – |
| Acarbose | – | – | – | – | 0.68 ± 0.02 [a] | 23.83 ± 0.55 [d] |

The results are expressed as mean ± standard deviation of six replicates. Means with different superscript letters are significantly different ($p < 0.05$). "-" indicates the activities were not measured due to the irrelevance to the compounds.

database, KNApSAcK, NMRDB, and Human Metabolome Database). Previously, phenolics (gallic acid and bergenin), flavonoids (myricetin, kaempferol, and myrigalone G), triterpenoids (lupeol, β-amyrin, and friedelin), and ellagitannins (castalagin, casuarinin, vescalagin, and dihexahydroxydiphenoyl (HHDP) glucose) were reported in the genus *Syzygium* (Sobeh et al., 2018). In the current study, 17 compounds comprising primary and secondary metabolites were further annotated *via* NMR (Table 2).

### 3.3. Discrimination of S. jambos leaf extracts

The generated principal component analysis (PCA) score plot investigates the impact of extraction solvent polarity on clustering characteristics. Besides, a corresponding loading plot (Fig. 1b) was applied to determine the metabolite variation among *S. jambos* leaf extracts. The PCA score plot (Fig. 1a) showed the two major PCs contributed to a total variance of 80.3 %, with PC1 (67.1 %) and PC2 (13.2 %). Based on the plot, *S. jambos* leaves extracted with different solvent systems were divided into four distinct clusters without visible outliers. PC1 separated the absolute ethanol extract from hydroethanolic and water extracts, while PC2 discriminated the 50 % and 70 % ethanolic extracts from the absolute and water extracts. Meanwhile, the loading plot (Fig. 1b) demonstrated that the hydroethanolic extracts shared similarities in metabolite retention and hence were closely clustered.

### 3.4. Metabolite correlation with biological activities

Partial least square (PLS) analysis was employed to further evaluate the relationship between biological activities and the identified metabolites of the *S. jambos* leaf extracts. The PLS biplot (Fig. 2) is a composition of both score and loading plots in a single graphical presentation (Abdul-Hamid et al., 2015), To avoid bias analysis, two separate PLS biplots were generated to investigate the correlation between the X (binned $^1$H NMR spectral data) variables and Y (DPPH• and NO• radical scavenging, anti-α-amylase, and anti-α-glucosidase assays) variables for the inverse position of the Y variables in the plot.

### 3.5. Relative quantification of bioactive compounds

13 shared metabolites of both biplots that are strongly contributed to the bioactivities (VIP value > 1.0) were relatively quantified to the concentration of TSP according to the respective binned $^1$H NMR spectral data (Fig. 3 and Table S1).

### 3.6. Metabolite profiling via UHPLC-MS/MS

The most active extract, i.e., the 70 % ethanolic *S. jambos* leaf extract, was further characterized for its phytochemicals *via* ultrahigh-performance liquid chromatography–tandem mass spectrometry (UHPLC-MS/MS). It is worth mentioning that a number of 59 metabolites were conditionally identified in the *S. jambos* leaf extract (Table 3). The annotation was accomplished on literature data comparison and quest for various online databases (MassBank, PubChem, Metabolomics Workbench, KNApSAcK, and HMDB). The total ion chromatogram demonstrated the extensive compounds discovered between 0 and 30 min (Fig. S6). Tannins and flavonoids accounted for 34 % and 24 % of the 59 identified metabolites, respectively. Other classes of identified metabolites include terpenoids, phenols, and fatty acids.

## 4. Discussion

The present study evaluated the bioactive phytoconstituents in *S. jambos* leaves exhibiting antidiabetic properties through *in-vitro* anti-hyperglycemic activities by providing a comprehensive profile using $^1$H NMR metabolomics and UHPLC-MS/MS techniques. Four different solvent extraction systems were investigated on the retention of potential bioactive metabolites from the plant matrix. Ultra-sonication is a non-thermal extraction technique used in this study as it facilitates effective extraction of phytoconstituents from plant matrix in a shorter duration, requires less solvent, produces higher yield and better retention of the bioactive compounds (Kumar et al., 2021). The higher yield of hydroethanolic *S. jambos* extracts may be attributed to the combination of solvents used in the extraction, which facilitated the solubility of both polar and less polar compounds from the plant matrices (Abdul-Hamid et al., 2015). The nonalignment of the TPC with the extraction yield might be attributed to the higher amount of non-phenol compounds such as terpenes and the carbohydrates being extracted in more polar solvents. In addition, complex formation of phenolic compounds can be possibly found in the extract, and these compounds may have more phenol groups than the more polar extracts (Do et al., 2014). Oxidative stress has been postulated in chronic diseases including diabetes (Lobo et al., 2010), thus, two *in-vitro* antioxidant activities, specifically 2,2-diphenyl-1-picrylhydrazyl (DPPH•) and nitric oxide (NO•), radical scavenging activities were conducted to evaluate the antioxidant potential of *S. jambos* leaf extracts. Interestingly, a different trend was observed in both antioxidant assays. This may be due to the different antioxidant mechanisms (Sumanont et al., 2004). In the DPPH• assay, antioxidants normally act by donating electron or hydrogen atoms to scavenge DPPH• free radicals, whereas the NO• radicals could be scavenged by receiving hydrogen atom from antioxidant or the formation of antioxidant cation with successive loss of hydrogen atom (Sumanont et al., 2004). Thus, this study suggested that the antioxidant potential of *S. jambos* leaf extracts is higher in DPPH• free radicals than in NO• free radicals.

Furthermore, the inhibition of two carbohydrate hydrolyzing enzyme activities, particularly anti-α-amylase and anti-α-glucosidase assays, was evaluated on the anti-hyperglycemic properties of *S. jambos* leaf extracts. A slightly different trend was discovered in the anti-α-amylase and anti-α-glucosidase activities, even though the most active extract is 70 % ethanolic extract and the water extract is the least active in both cases. This may be attributed to the distinct principle of the enzymatic reaction. During normal carbohydrate ingestion, the complex

**Table 2**
1D- and 2D-NMR characteristic signals of identified metabolites in *S. jambos* leaves extracted using 0%, 50%, 70% and absolute ethanol.

| No | Metabolites | $^{1}$H NMR characteristic signals | TOCSY correlations $\delta^{1}$H | HSQC correlations $\delta^{13}$C | HMBC correlations $\delta^{13}$C | 0 % EtOH | 50 % EtOH | 70 % EtOH | Abs EtOH |
|---|---|---|---|---|---|---|---|---|---|
| **Primary metabolites** | | | | | | | | | |
| 1 | α-Glucose | 5.18 (d, $J$ = 3.5 Hz) | – | – | – | + | + | + | + |
| 2 | β-Glucose | 4.57 (d, $J$ = 8 Hz) | – | – | – | + | + | + | + |
| 3 | Fructose | 4.10 (m) | – | – | – | + | + | + | – |
| 4 | Valine | 3.61 (d, $J$ = 5.0 Hz) | – | – | – | + | + | + | + |
| 5 | Alanine | 1.47 (d, $J$ = 7 Hz) | – | – | – | + | + | + | – |
| 6 | Formic acid | 8.47 (s) | – | – | – | + | – | – | – |
| 7 | Choline | 3.19 (s) | – | – | – | + | + | + | + |
| 8 | Gallic acid | 7.15 (s) | – | – | – | + | + | + | + |
| **Secondary metabolites** | | | | | | | | | |
| 9 | Stigmasterol | 5.10 (m)<br>1.03 (s) | – | – | – | + | + | + | + |
| 10 | Lupeol | 4.54 (s)<br>1.07(s)<br>0.94 (s) | – | – | – | – | + | + | + |
| 11 | Syringic acid | 7.33 (s)<br>3.82 (s) | – | – | – | + | + | + | + |
| 12 | β-amyrin | 2.03 (s)<br>1.04 (s)<br>0.86 (s) | – | – | – | + | + | + | + |
| 13 | Bergenin derivatives | 4.06 (s)<br>4.02 (dd, $J$ = 1.5, 12.0 Hz)<br>3.81 (m)<br>3.78 (m) | – | 74.53 (C8) | – | + | + | + | + |
| 14 | Myricetin derivatives | 7.05 (s)<br>6.31 (d, $J$ = 2.0 Hz) | – | – | – | + | + | + | + |
| 15 | Kaempferol derivatives | 8.04 (d, $J$ = 8.7 Hz)<br>6.74 (d, $J$ = 1.9 Hz)<br>6.42 (d, $J$ = 1.9 Hz)<br>6.29 (d, $J$ = 2.0 Hz) | 6.45 (H8) | 97.23 (C8)102.02 (C6) | – | + | + | + | + |
| 16 | Friedelin | 1.57 (m)<br>1.31 (m)<br>1.02 (s)<br>0.92 (d, $J$ = 6 Hz)<br>0.88 (s)<br>0.74 (s) | 1.57 (H18) | 18.73 (C26/27) | – | – | + | + | + |
| 17 | Stigmasterol glucoside | 4.51 (d, $J$ = 8 Hz)<br>3.72 (m)<br>3.58 (m)<br>2.03 (m)<br>1.35 (d, $J$ = 7.0 Hz)<br>1.06 (t, $J$ = 7.2 Hz)<br>0.93 (d, $J$ = 7.0 Hz) | – | 19.38 (C35) | – | – | + | + | + |
| 18 | Myrigalone G | 7.18 (m)<br>3.80 (s)<br>3.34 (t, $J$ = 8.0 Hz)<br>2.94 (t, $J$ = 8.0 Hz)<br>1.90 (s) | 3.34 (Hα) | 30.33 (Cβ) | – | – | + | + | + |
| 19 | Galloyl castalagin | 7.14 (s)<br>6.78 (s)<br>6.58 (s) | – | – | 112.66 (C21), 141.77 (C23), 148.16 (C20) | – | + | + | + |
| 20 | Casuarinin | 6.75 (s)<br>6.48 (s)<br>5.60 (d, $J$ = 5.0 Hz)<br>5.30 (d, $J$ = 7.0 Hz) | – | – | – | + | + | + | + |
| 21 | Tellimagrandin II | 7.16 (s)<br>7.11 (s)<br>7.01 (s)<br>3.80 (d, $J$ = 14 Hz) | – | 112.79 (C3′)<br>112.73 (C3) | 147.99 (C6),170.70 (C7) | – | + | + | + |
| 22 | Coriariin B | 7.35 (d, $J$ = 2.0 Hz)<br>7.23 (d, $J$ = 2.0 Hz)<br>7.00 (s)<br>6.98 (s)<br>6.65 (s)<br>6.49 (s) | – | – | – | + | + | + | + |
| 23 | Coriariin A | 6.70 (d, $J$ = 2.0 Hz)<br>6.98 (s)<br>6.68 (s)<br>6.65 (s) | – | – | – | + | + | + | + |
| 24 | Praecoxin A | 7.13 (s)<br>6.58 (s) | – | 110.90 (C3)110.03 (C6′′) | – | + | + | + | + |

(*continued on next page*)

**Table 2** (*continued*)

| No | Metabolites | $^{1}$H NMR characteristic signals | TOCSY correlations δ$^{1}$H | HSQC correlations δ$^{13}$C | HMBC correlations δ$^{13}$C | 0 % EtOH | 50 % EtOH | 70 % EtOH | Abs EtOH |
|---|---|---|---|---|---|---|---|---|---|
| | | 6.49 (s)<br>3.71 (d, *J* = 13 Hz) | | | | | | | |
| 25 | Praecoxin B | 7.11 (s)<br>6.39 (s)<br>5.18 (d, *J* = 3.5 Hz) | – | – | – | + | + | + | + |
| 26 | Vescalagin | 6.96 (s)<br>6.79 (s)<br>4.51 (d, *J* = 8 Hz)<br>4.18 (s) | – | 112.75 (C3′)<br>112.70<br>(C3) | 170.19 (C7),147.83 (C1)<br>,118.31<br>(C4) | + | + | + | + |
| 27 | Vescalin | 6.79 (s)<br>5.32 (s)<br>3.95 (t, *J* = 7 Hz)<br>3.88 (dd, *J* = 3, 12 Hz) | – | – | – | + | + | + | + |
| 28 | Trigalloyl glucose | 5.63 (d, *J* = 7.7 Hz)<br>5.26 (d, *J* = 7.7 Hz)<br>5.03 (m)<br>3.97 (d, *J* = 12.5) | – | – | – | + | + | + | + |
| 29 | Di-HHDP glucose | 7.49 (s)<br>6.65 (s)<br>5.34 (s)<br>5.18 (d, *J* = 3.5 Hz)<br>4.58 (d, *J* = 8 Hz)<br>3.70 (d, *J* = 12 Hz)<br>3.51<br>(d, *J* = 12 Hz) | – | 112.78 (C3′) | 172.88 (C7) | + | + | + | + |
| 30 | Pomolic acid | 3.46 (dd, *J* = 4.0, 11.0 Hz)<br>2.74 (s)<br>1.90 (s)<br>1.70 (m)<br>1.45 (m)<br>1.14 (d, *J* = 7.0 Hz)<br>1.07 (s)<br>0.92 (s) | 1.90 (H22)1.45 (H4) | 52.13 (C18′) | – | – | + | + | + |

"+" indicating presence and "-" indicating absence of the signals in the extracts.

starch structure is first hydrolyzed by α-amylase enzyme, which is further hydrolyzed by membrane-bound intestinal α-glucosidase enzyme to glucose and other monosaccharides for absorption (Alqahtani et al., 2020). In the anti-α-amylase assay, the DNS reagent detected and estimated the amount of reducing sugar as the product of enzymatic reaction, whereas in the anti-α-glucosidase assay, the potential to prevent enzyme from hydrolyzing the substrate for glucose production was evaluated (Miller, 1959). Thus, the inhibition of both α-amylase and α-glucosidase enzyme assays could suppress carbohydrate digestion, which could delay glucose uptake and reduce the blood glucose level. The positive results from *in-vitro* antioxidant and anti-hyperglycemic activities might justify the ethnobotanical use of *S. jambos* leaves in indigenous communities to treat diabetes and inflammatory-associated diseases. Furthermore, the *in-vitro* outcomes supported research on *in-vivo* models demonstrated antidiabetic properties of *S. jambos* bark and leaves in Type I diabetic model by protecting pancreatic β-cells against oxidative stress and enhancing insulin signaling pathway (Mahmoud et al., 2021). In view of this bioactive medicinal plant, *S. jambos* is considered harmless for consumption as its safety dose is up to 5 g/kg body weight in acute toxicity rat model evaluation (Dhanabalan et al., 2014). Different extracts and fractions of the leaves exhibited various toxicity levels on brine shrimp *Artemia salina* assay (Ochieng et al., 2022). However, there is limited information on the toxicological data of this plant to date which is yet to be fully explored.

The highly overlapping signals in the sugar region ($\delta$ 3.10–5.50) of the NMR spectra complicate the metabolite identification. The water extract exhibited a higher peak intensity in this region compared with the ethanolic extract, with signals at $\delta_H$ 5.18 (d, *J* = 3.5 Hz) and $\delta_H$ 4.57 (d, *J* = 8 Hz) could be annotated as α-glucose (**1**) and β-glucose (**2**), respectively. In the aliphatic region ($\delta$ 0.50–3.00), the water extract generated lesser peaks with lower concentration, interpreting the absence of lupeol (**10**), friedelin (**16**), stigmasterol glucoside (**17**), myrigalone G (**18**) and pomolic acid (**30**). In addition, the water extract did not increase galloyl castalagin (**19**) and tellimagrandin II (**21**) in the aromatic region ($\delta_H$ 5.00–8.50). Meanwhile, the primary metabolites were absent in the absolute ethanol extract including fructose (**3**) and alanine (**5**) (Khoo et al., 2015).

Based on the TOCSY spectrum, identification of kaempferol derivatives (**15**) was further supported by the correlation via spin–spin coupling at resonating signals at $\delta_H$ 6.29 and 6.42 in position H6 and H8 respectively in the aromatic A-ring of the structure. HSQC experiment also showed correlations of H6 to C6 at $\delta_c$ 102.02, and H8 to C8 at $\delta_c$ 97.23, indicating direct attachment of hydrogen atoms to carbon atoms in the compound. Besides, bergenin derivatives (**13**) could be characterized by a direct correlation of H8 ($\delta_H$ 4.02) to C8 at $\delta_c$ 74.53 by HSQC analysis. Besides, myrigalone G (**18**) could be further identified with TOCSY correlations of Hβ and Hα resonating at $\delta_H$ 2.94 and 3.34 respectively, where Hβ ($\delta_H$ 2.94) showed a direct correlation of HSQC experiment at $\delta_C$ 30.33 (Hβ-Cβ) (Jayasinghe et al., 2007).

Several ellagitannins could be further characterized using 2D-NMR experiments. HMBC analysis supported the structure of galloyl castalagin (**19**) by 3 J correlation between H21 ($\delta_H$ 7.14) of the galloyl moiety with C21 ($\delta_C$ 112.66), C23 ($\delta_C$ 141.77) and C20 ($\delta_C$ 148.16) of the aromatic ring in HHDP group (Yang et al., 2000). Galloyl moiety was anticipated attached to castalagin relatively higher compared to its isomer vescalagin, as galloyl castalagin was previously identified in *S. jambos* leaves (Ochieng et al., 2022). As for tellimagrandin II (**21**), proton at $\delta_H$ 7.11 (H3) and $\delta_H$ 7.18 (H3′) showed a direct correlation in the HSQC experiment at $\delta_C$ 112.73 (H3-C3) and $\delta_C$ 112.79 (H3′-C3′) of the HHDP moiety, while HMBC showed H3 correlate to C6 ($\delta_C$ 147.99) and C7 ($\delta_C$ 170.70). Furthermore, HSQC showed the direct correlation of proton H6′′ at $\delta_H$ 6.49 to C6′′ ($\delta_C$ 110.03) of the valoneoyl group, and H3 ($\delta_H$ 6.58) to C3 ($\delta_C$ 110.90) of HHDP moiety in praecoxin A (**24**). Vescalagin (**26**) showed HSQC correlation between H3 ($\delta_H$ 6.79) and C3 at

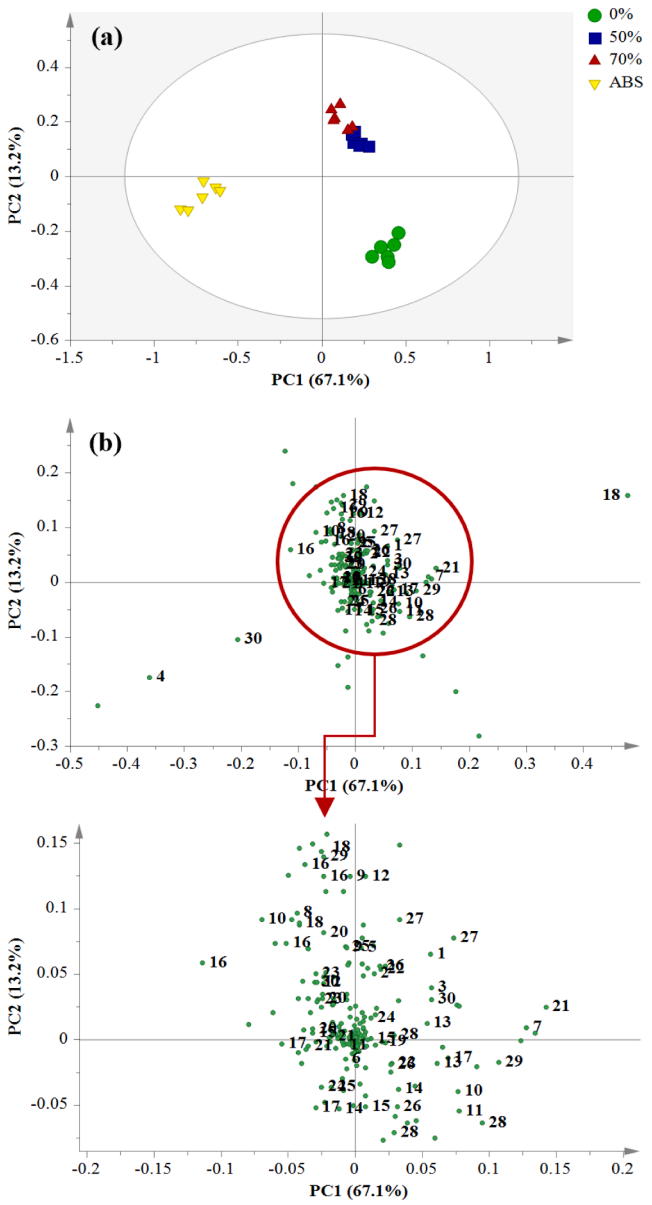


**Fig. 1.** **(a)** Principal component analysis (PCA) score plot and **(b)** Loading plot of *S. jambos* leaves extracted with 0%, 50%, 70% and absolute ethanol.

$\delta_C$ 112.70, while the correlation of H3 to C1 ($\delta_C$ 147.83), C4 ($\delta_C$ 118.31) and C7 ($\delta_C$ 170.19) were demonstrated in HMBC of D-ring and its carbonyl group of the structure. HSQC correlation demonstrates a direct correlation of H3′ ($\delta_H$ 6.96) to C3′ ($\delta_C$ 112.75) in the E-ring of the structure (Puech et al., 1999). The HHDP hydrogen in metabolite **29** showed a direct HSQC correlation of H3′ at $\delta_H$ 7.49 to C3′ at $\delta_C$ 112.78 of the aromatic ring, while a 3 J correlation of H3 ($\delta_H$ 6.65) to carbonyl carbon C7 at $\delta_C$ 172.88 could be assigned with HMBC experiment.

Identification of triterpenoids such as pomolic acid (**30**) was further strengthened by the TOCSY correlation of protons resonating at H16 ($\delta_H$ 1.70) and H22 ($\delta_H$ 1.90), H2 ($\delta_H$ 0.92), and H24 ($\delta_H$ 1.45), while a direct correlation of H18 ($\delta_H$ 2.74) to C18 at $\delta_C$ 52.13 could be assigned with HSQC experiment. Besides, identification of friedelin (**16**) was identified based on the hydrogen–hydrogen correlation in a spin system at $\delta_H$ 1.31 (H14) and $\delta_H$ 1.57 (H18), while a direct HSQC correlation could be assigned on H26/27 at $\delta_H$ 1.02 to C26/27 at $\delta_C$ 18.73 (Manguro et al., 2018).

Based on the identified metabolites, the discrimination of *S. jambos* leaves extracted by different solvent systems was manifested by the PCA score and loading plots, where less polar compounds, such as valine (**4**), friedelin (**16**), and pomolic acid (**30**), were more predominant in the absolute ethanol extract, and these metabolites positioned on the negative side of PC1. The water extract retained a higher amount of syringic acid (**11**), trigalloyl glucose (**28**), and di-HHDP glucose (**29**). Furthermore, the loading plot demonstrated that the hydroethanolic extracts had higher extraction of most metabolites, including myrigalone G (**18**), galloyl castalagin (**19**), casuarinin (**20**), tellimagrandin II (**21**), praecoxin A (**24**), praecoxin B (**25**), vescalagin (**26**), vescalin (**27**), and β-amyrin (**12**). This may be attributed to the use of a solvent mixture that is more effective in the dissolution of metabolites from plant matrices and possibly contribute to biological activities (Abdul-Hamid et al., 2015). The plot was validated with five evaluated principal components (PCs), with R2X (cum) = 0.949 and Q2 (cum) = 0.863. The difference between Q2 and R2X is less than 0.3 (0.086), indicating that the generated model is reliable and gained a strong predictive power (Khoo et al., 2015).

Biplot (a) (Fig. 2) shows the correlation of the metabolites with DPPH• radical scavenging activity, affording PC1 (67.1 %) and PC2 (7.7 %) of the total variance. The biplot showed that PC1 clearly separates the absolute ethanol extract from the hydroethanolic and water extracts, while the water extract is closely associated to the DPPH• activity. The plot was aligned with the bioactivities result in the current study, in which the water extract exhibited the highest DPPH• radical scavenging activity, and the lowest was absolute ethanol extract in the particular case. Meanwhile, the metabolites contributing to the DPPH• activity with variable importance in the projection (VIP) values higher than 1.0 including mostly flavonoids and some tannins such as syringic acid (**11**), bergenin (**13**), myricetin (**14**), and kaempferol (**15**) derivatives, myrigalone G (**18**), tellimagrandin II (**21**), coriariin B (**22**), vescalagin (**26**), vescalin (**27**), trigalloyl glucose (**28**), di-HHDP glucose (**29**), and several primary metabolites, including α-glucose (**1**), fructose (**3**), valine (**4**), and choline (**7**). The presence of free and glycosylated flavonoids in the extracts could strengthen antioxidant activity (Pereira et al., 2018). In contrast, the contradiction of high phenolic content with low DPPH• antioxidant power of the absolute ethanol extract in the present study might be explained by the chemical structure of phenolic compounds, including the number and position of hydroxyl groups that possibly influence the antioxidant capacity of the leaf extracts (Rice-Evans et al., 1996).

Another PLS biplot (b) (Fig. 2) was generated to examine the correlation of the metabolites with NO• radical scavenging, anti-α-amylase, and anti-α-glucosidase activities, affording PC1 (59.8 %) and PC2 (19.9 %) of the total variance. The biplot showed that PC1 separated the 70 % ethanolic and absolute ethanol extracts from the 50 % ethanolic and water extracts, while PC2 discriminated the hydroethanolic extracts from the water and absolute ethanol extracts. The 70 % ethanolic extract was found to be closely correlated with the biological activities, which is aligned with the bioactivities result in the current study. Furthermore, metabolite signals with VIP values > 1.0 indicate potential X variables granted to this model. For instance, most of the tannins, including myrigalone G (**18**), tellimagrandin II (**21**), coriariin A (**23**), praecoxin A (**24**), praecoxin B (**25**), vescalin (**27**), trigalloyl glucose (**28**), and di-HHDP glucose (**29**), contribute to the biological activities. Tannins isolated in the genus *Syzygium* have been previously reported to exhibit antioxidant and anti-hyperglycemic properties that strengthen the current PLS biplot (Gavillán-suárez et al., 2015; Sobeh et al., 2018). Several phenolic compounds, including bergenin derivatives (**13**) and gallic acid (**8**), also contributed to the activities.

Interestingly, a total of 13 metabolites shared between both biplots contributed significantly (VIP value > 1.0) to the antioxidant and anti-hyperglycemic activities of the *S. jambos* leaf extracts. Among these bioactive compounds, five tannins (di-HHDP glucose (**29**), myrigalone G (**18**), tellimagrandin II (**21**), trigalloyl glucose (**28**), and vescalin (**27**)) and three triterpenoids (pomolic acid (**30**), friedelin (**16**), and lupeol (**10**)) were found to be highly associated with the bioactivities.

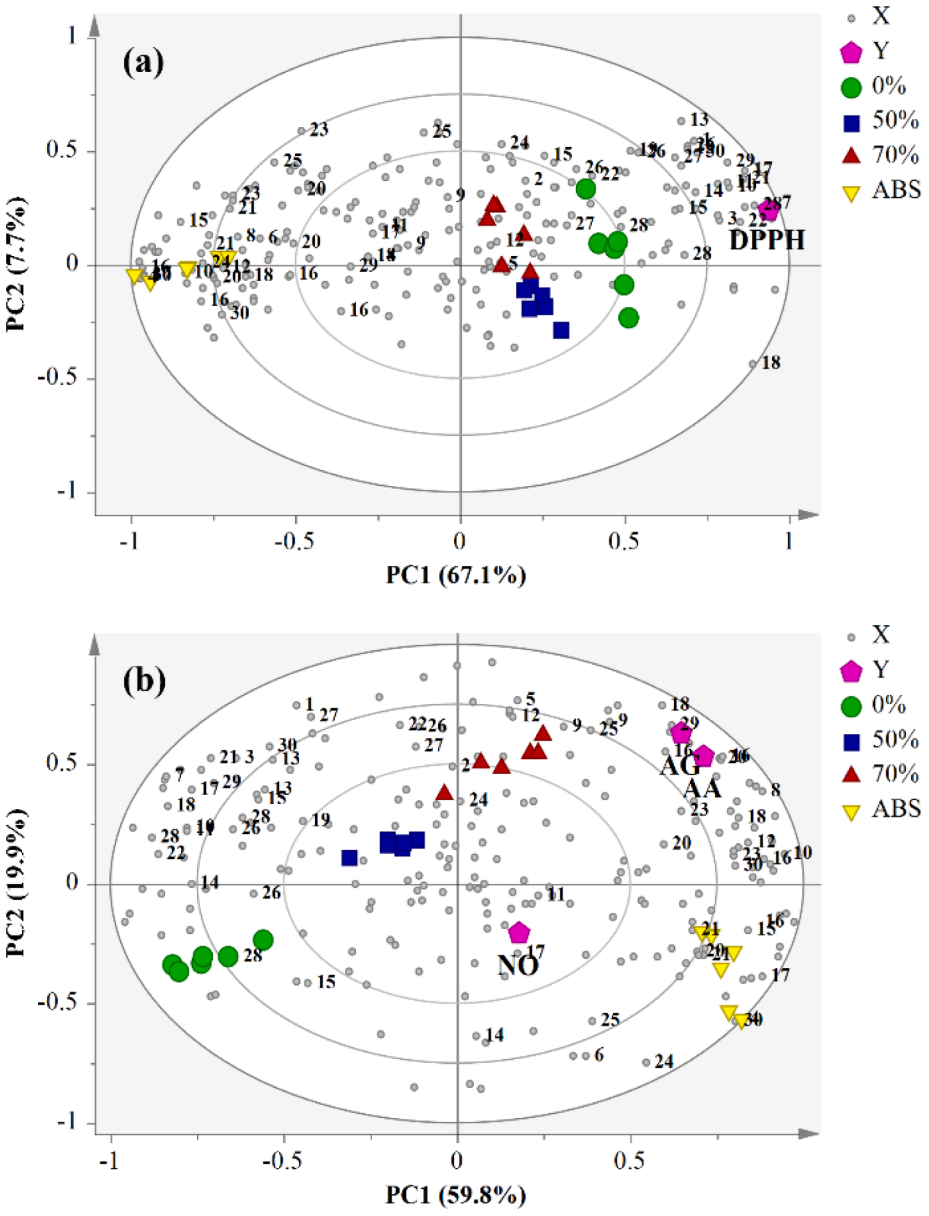


**Fig. 2.** Partial least square (PLS) biplot illustrating the correlation of metabolites in *S. jambos* leaves with **(a)** DPPH• activity, **(b)** NO•, anti-α-amylase and anti-α-glucosidase activities; AA: anti-α-amylase, AG: anti-α-glucosidase.

Moreover, bergenin derivatives (**13**), stigmasterol glucoside (**17**), and several primary metabolites, including choline (**7**), valine (**4**), and α-glucose (**1**), also strongly correlated with the bioactivities. Valine is known to be involved in the shikimate pathway for the biosynthesis of phenolic acids, which explains the significant contribution to the activity as observed in the model (Pramai et al., 2018). These significantly contributing metabolites in *S. jambos* leaves to antioxidant and anti-hyperglycemic activities revealed by PLS analysis substantially justified the traditional use of *S. jambos* leaves for treating diabetes and various inflammatory-associated illnesses.

Both PLS models were verified using the internal cross-validation technique. Two PCs with R2Y (cum) = 0.935 and Q2 = 0.901 and five PCs with R2Y (cum) = 0.98 and Q2 = 0.913 were evaluated in biplots (a) and (b), respectively. This indicated that the models were statistically valid. Furthermore, the permutation test (Fig. S7) was employed to further validate the models in order to explain the overfitting degree and predictive ability. Both models obtained Y-intercepts of R2 (<0.4) and Q2 (<0.05), indicating the robustness and reliability of the PLS models (Eriksson et al., 2006). In addition, the models were also validated by regression analysis, with the r values of DPPH•, NO•, anti-α-amylase, and anti-α-glucosidase assays being 0.9351, 0.6886, 0.9305, and 0.9817, respectively (Fig. S8). Overall, the PLS models were statistically validated and are thus reliable.

The bioactive metabolites were relatively quantified where the water extract retained a higher amount of bergenin derivatives, choline, and several tannins, including di-HHDP glucose and vescalin, without significant difference with 70 % ethanolic extract. Meanwhile, the 70 % ethanolic extract contained a significantly higher concentration of myrigalone G, tellimagrandin II, and α-glucose compared with the other extracts. Less polar compounds, such as friedelin, lupeol, pomolic acid, and valine, are significantly predominant in the absolute ethanol extract. It is important to note that both hydroethanolic extracts contained most of the metabolites, such as choline, lupeol, myrigalone G, trigalloyl glucose, and valine without significant difference. These findings agree with those of the PCA and PLS analysis in the present study, in which the solubilization of bioactive compounds from *S. jambos* leaves was influenced by the polarity of the solvent used in the extraction.

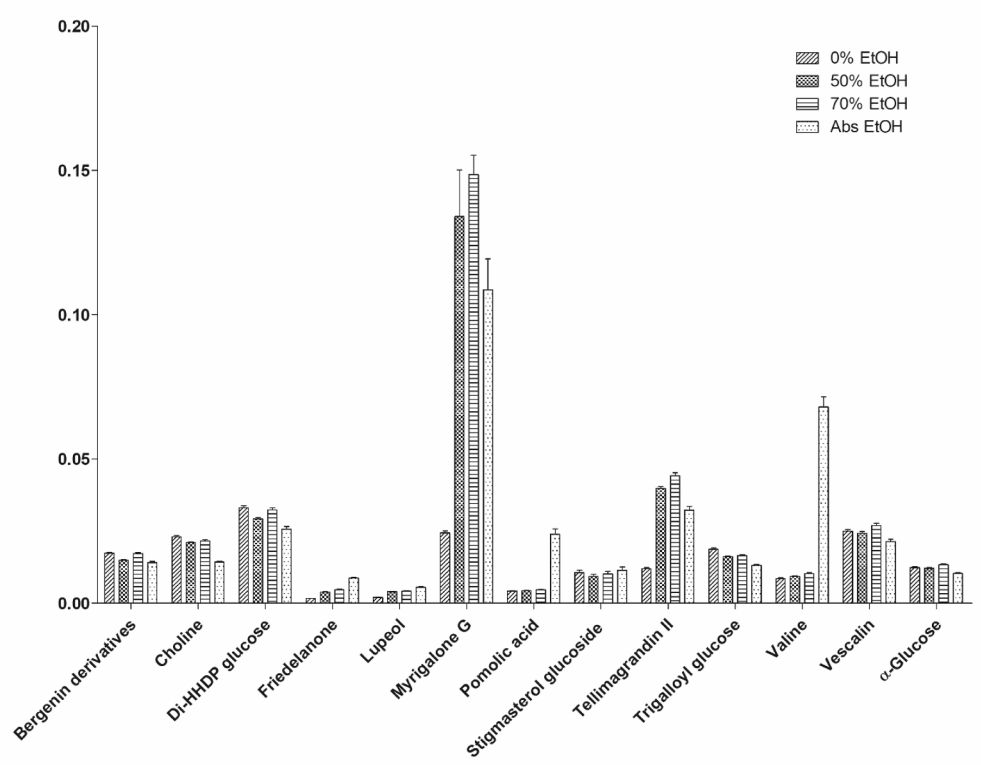


**Fig. 3.** Relative quantification of the identified metabolites in *S. jambos* leaves extract.

In view of the contribution of *S. jambos* leaves' bioactive phytochemicals to the antioxidants and anti-hyperglycemic activities, a higher sensitivity of the MS technique was applied to detect low-abundance metabolites that might appear to be invisible and ambiguous in NMR due to its shortcoming. Hydrolyzable tannins including ellagitannins and gallotannins are major polyphenolic compounds identified in the *S. jambos* leaf extract. Gallotannins comprised of polyesters of sugar moiety and gallic acid; where ellagitannins contained hexahydroxydiphenic acid (HHDP) ester which metabolically derived from gallotannins (Plaza et al., 2016). The radicals scavenging capacity of hydrolyzable tannins depends on molecular size, as a higher number of galloyl and HHDP groups in the molecule enhanced radicals scavenging activities by the formation of stable quinone (Valverde Malaver et al., 2019). Several hydrolyzable ellagitannins identified including strictinin and eugeniin were previously identified in the genus *Syzygium*, which could be annotated in this study. Strictinin (**39**) was identified based on fragment ions at *m/z* 463 and 300, which correspond to the cleavage of gallic acid (169 u) and glucosyl moiety (162 u) from the deprotonated molecular ion at *m/z* 633.0724 (Taamalli et al., 2013). Eugeniin or tellimagrandin II (**21**) was identified based on the deprotonated molecular ion at *m/z* 937.0940 with fragment ions at *m/z* 785, 635, and 483 due to the subsequent loss of three galloyl moieties (152 u) and 300, which is consistent with a previously reported MS/MS data (Grace et al., 2014). Furthermore, both tellimagrandin I (**47**) and casuarinin (**20**) could be observed with the loss of subsequent galloyl moieties (152 u) to yield fragment ions at *m/z* 783, 633, and 483 from deprotonated molecular ions at *m/z* 785.0833 and 935.0798, respectively (Díaz-de-Cerio et al., 2016). Gallotannins, such as digalloyl glucose isomers (**32**, **34**, **35**, **36**, **43** and **45**), were tentatively identified based on deprotonated molecular ion at *m/z* 483.0775 and fragment ion at *m/z* 331, which correspond to a galloyl glucose molecule, 313 and 169, based on the subsequent loss of hydroxyl and glucose moieties, respectively (Slatnar et al., 2015). Moreover, ellagitannins, such as di-HHDP glucose and its isomers (**29**, **37**, **41**, **42**), could be identified based on deprotonated molecular ion at *m/z* 783.0673 and fragmentation patterns at *m/z* 481 (loss of HHDP), 300 (elimination of HHDP-glucose), and the corresponding fragments to the HHDP unit at *m/z* 275, 257, and 229, which the experimental fragment pattern is in agreement with previous study (Plaza et al., 2016). Other polyphenols, such as citric acid (**33**), ellagic acid (**57**), and its derivative (**50**), could be detected in the *S. jambos* leaf extract (Lantzouraki et al., 2015; Regueiro et al., 2014).

Apart from hydrolyzable tannins, flavonoids were identified as another major class of compounds in *S. jambos* leaf extract. Hydroxyl configuration of the B ring of flavonoids is the most significant factor in radicals scavenging capacity as it provides a greater stability for flavonoid radical formation. Furthermore, antioxidant activities were influenced by the occurrence and number of glycoside moieties in flavonoids (Kumar & Pandey, 2013). A total of seven quercetin derivatives were relatively annotated in the *S. jambos* leaf extract, based on the characteristic aglycone fragment ion at *m/z* 301. Quercetin glucuronide (**49**) could be identified based on deprotonated molecular ion at *m/z* 477.0663 and fragment ions at *m/z* 300 due to the loss of glucuronide moiety (177 u). Peaks **59**, **61**, **62**, and **63** were assigned as quercetin glucoside, quercetin arabinoside, quercetin rhamnoside, and quercetin xylosyl-rhamnoside with the deprotonated molecular ions at *m/z* 463.0875, 433.0774, 447.0928, and 579.1348, respectively (Lee et al., 2019). These metabolites were identified according to their corresponding loss of arabinosyl (132 u), rhamnosyl (146 u), xylosyl (150 u), and glucose (162 u) residues to yield quercetin aglycone. Furthermore, myricetin derivatives could be identified in the extract as myricetin glucoside (**52**), myricetin robinobioside (**56**), and myricetin xylosyl-rhamnoside (**58**) based on the presence of characteristic myricetin aglycone fragment ion at *m/z* 316 (Lee et al., 2019). Other flavonoids, such as jaceidin rhamnoside (**60**), could be identified based on deprotonated molecular ion at *m/z* 505.1351 and fragment ions at *m/z* 359 (loss of rhamnosyl moiety), 344 (loss of methyl group), and 329 after subsequent deduction of two methyl groups (Taamalli et al., 2013).

Triterpenoids were annotated in the *S. jambos* leaf extract, including pomolic acid (**30**) and maslinic acid (**79**). Both metabolites shared virtually similar deprotonated molecular weight at *m/z* 471.3469 and

**Table 3**
Mass spectral characteristics and tentative identification of compounds present in 70% ethanolic leaves extract of *S. jambos*.

| Peak no. | Retention time, min | Exact mass | Deprotonated molecular ion $[M-H]^-$ (*m/z*) | Delta | MS/MS fragment ions | Tentative identification | Molecular formula | References |
|---|---|---|---|---|---|---|---|---|
| 31 | 0.64 | 504.1618 | 503.1611 | 0.0007 | 221.0659, 179.0549, 161.0443, 113.0230, 101.0230 | Raffinose | $C_{18}H_{32}O_{16}$ | (Kubica et al., 2012) |
| 32 | 0.72 | 484.0780 | 483.0775 | 0.0005 | 331.0666, 313.0343, 300.9986, 169.0129 | Digalloyl glucose | $C_{20}H_{20}O_{14}$ | (Slatnar et al., 2015) |
| 33 | 0.99 | 192.0197 | 191.0187 | 0.0010 | 173.0079, 129.0180, 111.0074, 87.0073, 85.0281 | Citric acid | $C_6H_8O_7$ | (Lantzouraki et al., 2015) |
| 34 | 1.02 | 484.0780 | 483.0775 | 0.0005 | 331.0666, 313.0343, 300.9985, 169.0130 | Digalloyl glucose isomer 1 | $C_{20}H_{20}O_{14}$ | (Slatnar et al., 2015) |
| 35 | 1.61 | 484.0780 | 483.0776 | 0.0004 | 331.0666, 313.0343, 300.9985, 169.0131 | Digalloyl glucose isomer 2 | $C_{20}H_{20}O_{14}$ | (Slatnar et al., 2015) |
| 36 | 1.74 | 484.0780 | 483.0776 | 0.0004 | 331.0666, 313.0343, 300.9986, 169.0129 | Digalloyl glucose isomer 3 | $C_{20}H_{20}O_{14}$ | (Slatnar et al., 2015) |
| 29 | 2.21 | 784.0681 | 783.0674 | 0.0007 | 481.0626, 300.9984, 275.0193, 257.0088, 229.0136 | Di-HHDP glucose | $C_{34}H_{24}O_{22}$ | (Plaza et al., 2016) |
| 26 | 2.29 | 934.0640 | 933.0623 | 0.0017 | 915.0509, 631.0547, 467.0239, 451.0322, 300.9985 | Vescalagin | $C_{41}H_{26}O_{26}$ | (Sobeh et al., 2018) |
| 37 | 2.55 | 784.0681 | 783.0673 | 0.0008 | 481.0626, 300.9984, 275.0193, 257.0088, 229.0136 | Di-HHDP glucose isomer 1 | $C_{34}H_{24}O_{22}$ | (Plaza et al., 2016) |
| 38 | 2.86 | 934.0640 | 933.0631 | 0.0009 | 631.0565, 467.0230, 451.0292, 300.9985 | Vescalagin isomer | $C_{41}H_{26}O_{26}$ | (Sobeh et al., 2018) |
| 39 | 3.06 | 634.0734 | 633.0724 | 0.0010 | 463.0522, 300.9985, 275.0193 | Strictinin | $C_{27}H_{22}O_{18}$ | (Taamalli et al., 2013) |
| 40 | 3.11 | 634.0734 | 633.0724 | 0.0010 | 463.0508, 300.9985, 275.0193 | Strictinin isomer 1 | $C_{27}H_{22}O_{18}$ | (Taamalli et al., 2013) |
| 41 | 3.34 | 784.0681 | 783.0673 | 0.0008 | 481.0597, 300.9986, 275.0194, 257.0089, 229.0135 | Di-HHDP glucose isomer 2 | $C_{34}H_{24}O_{22}$ | (Plaza et al., 2016) |
| 42 | 3.39 | 784.0681 | 783.0670 | 0.0011 | 481.0597, 300.9986, 275.0194, 257.0083, 229.0135 | Di-HHDP glucose isomer 3 | $C_{34}H_{24}O_{22}$ | (Plaza et al., 2016) |
| 43 | 3.78 | 484.0780 | 483.0773 | 0.0007 | 331.0666, 313.0561, 300.9980, 169.0131 | Digalloyl glucose isomer 4 | $C_{20}H_{20}O_{14}$ | (Slatnar et al., 2015) |
| 44 | 3.88 | 1068.1213 | 1067.1205 | 0.0008 | 533.0539, 377.0291, 300.9987, 249.0396 | Pterocarinin A | $C_{46}H_{36}O_{30}$ | (Díaz-de-Cerio et al., 2016) |
| 45 | 3.93 | 484.0780 | 483.0772 | 0.0008 | 331.0666, 313.0561, 300.9988, 169.0131 | Digalloyl glucose isomer 5 | $C_{20}H_{20}O_{14}$ | (Slatnar et al., 2015) |
| 46 | 4.12 | 634.0734 | 633.0725 | 0.0009 | 463.0503, 300.9986, 275.0194 | Strictinin isomer 2 | $C_{27}H_{22}O_{18}$ | (Taamalli et al., 2013) |
| 20 | 4.29 | 936.0796 | 935.0798 | 0.0002 | 783.0668, 633.0737, 481.0637, 300.9991, 275.0195, 169.0131 | Casuarinin | $C_{41}H_{28}O_{26}$ | (Díaz-de-Cerio et al., 2016) |
| 47 | 4.56 | 786.0843 | 785.0833 | 0.0010 | 633.0725, 483.0795, 300.9985, 275.0193, 169.0132 | HHDP-digalloylglucose (Tellimagrandin I) | $C_{34}H_{26}O_{22}$ | (Plaza et al., 2016) |
| 48 | 4.70 | 306.0667 | 305.0696 | 0.0029 | 286.9944, 269.9857, 108.0201 | (-)-Epigallocatechin | $C_{15}H_{14}O_7$ | (Savić et al., 2014) |
| 49 | 5.00 | 478.0675 | 477.0663 | 0.0012 | 300.9986, 257.0090, 229.0137, 151.0027 | Quercetin glucuronide | $C_{21}H_{18}O_{13}$ | (Lee et al., 2019) |
| 50 | 5.10 | 464.0591 | 463.0581 | 0.0010 | 300.9982, 257.0091, 229.0127, 185.0236 | Ellagic acid hexoside | $C_{20}H_{16}O_{13}$ | (Slatnar et al., 2015) |
| 51 | 5.45 | 936.0796 | 935.0779 | 0.0017 | 633.0726, 481.0623, 300.9985, 275.0193, 169.0130 | Casuarinin isomer (Casuarictin) | $C_{41}H_{28}O_{26}$ | (Díaz-de-Cerio et al., 2016) |
| 52 | 5.70 | 480.0831 | 479.0823 | 0.0008 | 317.0269, 316.0220, 271.0242 | Myricetin glucoside | $C_{21}H_{20}O_{13}$ | (Lee et al., 2019) |
| 53 | 5.79 | 480.0831 | 479.0823 | 0.0008 | 317.0269, 316.0220, 271.0242 | Myricetin glucoside isomer | $C_{21}H_{20}O_{13}$ | (Lee et al., 2019) |
| 21 | 5.85 | 938.0953 | 937.0940 | 0.0013 | 785.0770, 635.0892, 483.0781, 300.9985 | Eugeniin / Tellimagrandin II | $C_{41}H_{30}O_{26}$ | (Grace et al., 2014) |
| 54 | 5.95 | 434.0776 | 433.0774 | 0.0002 | 300.9980, 283.9954, 271.9956 | Quercetin xyloside | $C_{20}H_{18}O_{11}$ | (Lee et al., 2019) |
| 55 | 6.10 | 616.0992 | 615.0989 | 0.0003 | 463.0880, 300.0273, 271.0237, 255.0295, 178.9976, 169.0132 | Quercetin galloylglucoside | $C_{28}H_{24}O_{16}$ | (Lee et al., 2019) |
| 56 | 6.19 | 626.1410 | 625.1406 | 0.0004 | 316.0220, 287.0195, 271.0244, 178.9977, 151.0023 | Myricetin robinobioside | $C_{27}H_{30}O_{17}$ | (Lee et al., 2019) |

(*continued on next page*)

**Table 3** (*continued*)

| Peak no. | Retention time, min | Exact mass | Deprotonated molecular ion $[M-H]^-$ (*m/z*) | Delta | MS/MS fragment ions | Tentative identification | Molecular formula | References |
|---|---|---|---|---|---|---|---|---|
| 57 | 6.42 | 301.9990 | 300.9981 | 0.0009 | 283.9954, 257.0089, 229.0135, 185.0235 | Ellagic acid | $C_{14}H_6O_8$ | (Regueiro et al., 2014) |
| 58 | 6.55 | 596.1305 | 595.1300 | 0.0005 | 316.0219, 287.0195, 271.0243, 178.9973, 151.0024 | Myricetin xylosyl-rhamnoside | $C_{26}H_{28}O_{16}$ | (Lee et al., 2019) |
| 59 | 6.64 | 464.0882 | 463.0875 | 0.0007 | 300.0272, 271.0244, 255.0299, 178.9974, 151.0025 | Quercetin glucoside | $C_{21}H_{20}O_{12}$ | (Lee et al., 2019) |
| 60 | 7.00 | 506.1352 | 505.1351 | 0.0001 | 359.1493, 344.1259, 329.1021, 300.0955 | Jaceidin rhamnoside | $C_{24}H_{26}O_{12}$ | (Taamalli et al., 2013) |
| 61 | 7.08 | 434.0776 | 433.0774 | 0.0002 | 300.0271, 271.0245, 255.0296, 178.9992, 151.0028 | Quercetin arabinoside | $C_{20}H_{18}O_{11}$ | (Lee et al., 2019) |
| 62 | 7.21 | 448.0933 | 447.0928 | 0.0005 | 301.9967, 300.9941, 270.9876, 255.5956 | Quercetin rhamnoside | $C_{21}H_{20}O_{11}$ | (Lee et al., 2019) |
| 63 | 7.41 | 580.1356 | 579.1348 | 0.0008 | 429.0834, 300.0272, 271.0245, 255.0295 | Quercetin xylosyl-rhamnoside | $C_{26}H_{28}O_{15}$ | (Lee et al., 2019) |
| 64 | 8.15 | 564.1406 | 563.1401 | 0.0005 | 413.0867, 285.0372, 255.0294, 227.0342, 178.9976, 151.0024 | Kaempferol rhamnoside-xyloside | $C_{26}H_{28}O_{14}$ | (Lee et al., 2019) |
| 65 | 8.87 | 478.1002 | 477.1031 | 0.0029 | 331.0663, 313.0565, 169.0131 | Gallic acid coumaroyl-hexose | $C_{22}H_{22}O_{12}$ | (Sobeh et al., 2018) |
| 66 | 11.18 | 328.2177 | 327.2170 | 0.0007 | 229.1440, 211.1331, 171.1015 | Trihydroxy octadecadienoic acid | $C_{18}H_{32}O_5$ | (Taamalli et al., 2013) |
| 67 | 11.96 | 330.2334 | 329.2327 | 0.0007 | 312.9938, 293.2107, 242.3922, 229.1438, 211.1331, 183.1379 | Trihydroxy octadecenoic acid | $C_{18}H_{34}O_5$ | (Taamalli et al., 2013) |
| 68 | 12.47 | 504.3378 | 503.3371 | 0.0007 | 485.3265, 453.3004, 427.3229, 407.2961, 370.8087, 174.9547 | Madecassic acid | $C_{30}H_{48}O_6$ | (Xia et al., 2015) |
| 69 | 13.20 | 504.3378 | 503.3373 | 0.0005 | 485.3270, 453.3011, 407.2961, 369.7016 | Madecassic acid isomer | $C_{30}H_{48}O_6$ | (Xia et al., 2015) |
| 70 | 15.29 | 488.3429 | 487.3415 | 0.0014 | 419.2439, 409.3099, 377.0679, 373.9642, 151.4273 | Asiatic acid | $C_{30}H_{48}O_5$ | (Xia et al., 2015) |
| 71 | 18.11 | ND | 723.3798 | ND | 695.0396, 415.1442, 279.2323 | Fatty acid derivative | ND | (Minkler & Hoppel, 2010) |
| 72 | 18.26 | ND | 476.2773 | ND | 416.2551, 279.2325, 214.0470, 196.0373 | Fatty acid derivative | ND | (Hsu et al., 2007) |
| 73 | 18.39 | ND | 564.3293 | ND | 505.3116, 279.2323, 481.8533 | Fatty acid derivative | ND | (Hsu et al., 2007) |
| 74 | 18.62 | ND | 559.3112 | ND | 496.2796, 412.5738, 277.2167 | Fatty acid derivative | ND | (Hsu et al., 2007) |
| 75 | 18.88 | ND | 699.3796 | ND | 437.1535, 415.1462, 255.2323, 172.3546 | Fatty acid derivative | ND | (Hsu et al., 2007) |
| 76 | 19.00 | ND | 452.2773 | ND | 255.2325, 214.0476, 196.0372 | Fatty acid derivative | ND | (Hsu et al., 2007) |
| 77 | 19.16 | ND | 540.3295 | ND | 436.6639, 417.5592, 255.2324 | Fatty acid derivative | ND | (Hsu et al., 2007) |
| 78 | 19.46 | ND | 431.2196 | ND | 294.7976, 277.2172, 171.0053 | Fatty acid derivative | ND | (Hsu et al., 2007) |
| 30 | 19.92 | 472.3480 | 471.3469 | 0.0011 | 454.1732, 427.1954, 393.3149, 246.9636, 201.9723 | Pomolic acid | $C_{30}H_{48}O_4$ | (Guo et al., 2011) |
| 79 | 20.15 | 472.3480 | 471.3470 | 0.0010 | 454.1732, 427.1954, 264.9446, 246.9636, 146.4775 | Maslinic acid | $C_{30}H_{48}O_4$ | (Cheng & Cao, 1992) |
| 80 | 23.19 | 456.3531 | 455.3525 | 0.0006 | 406.6367, 378.5817, 327.2702, 231.1748 | Oleanolic acid | $C_{30}H_{48}O_3$ | (Song et al., 2006) |
| 81 | 26.15 | 592.2613 | 591.2598 | 0.0015 | 559.2346, 515.2444, 500.2210, 487.2533, 460.2217 | Pheophorbide A | $C_{35}H_{36}N_4O_5$ | (Park et al., 2003) |
| 82 | 26.39 | 356.3218 | 355.3209 | 0.0009 | 338.3106, 309.3160, 295.2102, 280.1995, 254.8060, 238.9417, 102.1235 | Hydroxy-docosanoic acid | $C_{22}H_{44}O_3$ | (Muchembled et al., 2005) |
| 83 | 26.85 | 370.3447 | 369.3410 | 0.0037 | 353.1471, 325.2532, 309.2224 | Methyl hydroxydocosanoate | $C_{23}H_{46}O_3$ | (Gorst-Allman & Spiteller, 1988) |
| 84 | 27.01 | 370.3447 | 369.3410 | 0.0037 | 353.1471, 325.2532, 309.2224 | Methyl hydroxydocosanoate isomer | $C_{23}H_{46}O_3$ | (Gorst-Allman & Spiteller, 1988) |

fragmentation patterns at *m/z* 454 (loss of hydroxyl group), 427 (loss of carboxyl group, 44 u), and 393 (loss of hydroxyl, carboxyl, and methyl moieties). Nevertheless, metabolite **30** was identified as pomolic acid and the later eluted metabolite as maslinic acid (**79**) based on the elution order (Cheng & Cao, 1992; Guo et al., 2011). In addition, madecassic acid (**68**) was identified based on deprotonated molecular ion at *m/z* 503.3371 and fragment ions at 485 (loss of $H_2O$), 453 (subsequent loss of $HCH_2OH$), 407 (loss of HCOOH, $HCH_2OH$, and $H_2O$), 370, and 174, which is consistent with previous data (Xia et al., 2015). Asiatic acid (**70**) was identified with deprotonated molecular ion at *m/z* 487.3415 and fragment ions at *m/z* 419, 409 (loss of HCOOH and $HCH_2OH$), 377 (subsequent loss of $HCH_2OH$), 373, and 151 (Xia et al., 2015). Application of UHPLC-MS/MS further strengthened the metabolites identification providing a comprehensive phytochemical characterization of *S. jambos* leaf extract.

## 5. Conclusion

In conclusion, the present study provides a comprehensive insight into the *Syzygium jambos* leaf extracts with different solvent polarities in the retention of bioactive compounds. The application of $^1$H NMR metabolomics and ultrahigh-performance liquid chromatography-tandem mass spectrometry (UHPLC-MS/MS) allowed the detailed identification of metabolites in *S. jambos* leaves and the correlation with biological activities, demonstrating distinct clusters among the extracts with various ethanol concentrations. A total of 59 and 30 metabolites were identified *via* UHPLC-MS/MS and NMR, respectively. The PLS model demonstrated 13 bioactive compounds, including tannins, triterpenoids, and flavonoids, which may significantly contribute to the antioxidant and anti-hyperglycemic activities. This study provides the first comprehensive insights into *S. jambos* metabolome and serves as a reference for the use of an ingredient in functional food development. Future research into the absolute quantification of bioactive compounds in active extracts and the underlying mechanisms involved will be valuable. However, extensive dose- and time-repetitive toxicity studies were recommended to further validate the safety of this plant.

## CRediT authorship contribution statement

**Pei Lou WONG:** Data curation, Formal analysis, Investigation, Methodology, Software, Writing – original draft. **Nurul Shazini RAMLI:** Conceptualization, Project administration, Supervision. **Chin Ping TAN:** Methodology, Software, Supervision, Validation. **Azrina AZLAN:** Conceptualization, Project administration, Supervision. **Faridah ABAS:** Conceptualization, Funding acquisition, Project administration, Resources, Supervision, Validation, Visualization, Writing – review & editing.

## Declaration of Competing Interest

The authors declare that they have no known competing financial interests or personal relationships that could have appeared to influence the work reported in this paper.

## Acknowledgements

The authors wish to thank Universiti Putra Malaysia for the grant (GP-IPS/2021/9699000) provided under the Putra Graduates Initiative Grant Scheme. The first author also gratefully acknowledges the support from Universiti Putra Malaysia for funding her study under the Graduate Research Fellowship scheme.

## Appendix A. Supplementary material

Supplementary data to this article can be found online at https://doi.org/10.1016/j.arabjc.2023.105546.

## References

Abdul-Hamid, N.A., Abas, F., Ismail, I.S., Tham, C.L., Maulidiani, M., Mediani, A., Swarup, S., Umashankar, S., Zolkeflee, N.K.Z., 2019. Metabolites and biological activities of *Phoenix dactylifera* L. pulp and seeds: A comparative MS and NMR based metabolomics approach. Phytochem. Lett. 31, 20–32.

Abdul-Hamid, N.A., Abas, F., Ismail, I.S., Shaari, K., Lajis, N.H., 2015. Influence of different drying treatments and extraction solvents on the metabolite profile and nitric oxide inhibitory activity of Ajwa dates. J. Food Sci. 80(11), H2603–H2611.

Alqahtani, A.S., Hidayathulla, S., Rehman, M.T., Elgamal, A.A., Al-Massarani, S., Razmovski-Naumovski, V., Alqahtani, M.S., El Dib, R.A., Alajmi, M.F., 2020. Alpha-amylase and alpha-glucosidase enzyme inhibition and antioxidant potential of 3-oxolupenal and katononic acid isolated from *Nuxia oppositifolia*. Biomolecules 10 (61), 1–19.

Avila-Pena, D., Pena, N., Quintero, L., Suarez-Roca, H., 2007. Antinociceptive activity of *Syzygium jambos* leaves extract on rats. J. Ethnopharmacol. 112, 380–385.

Baliga, M.S., Ranganath Pai, K.S., Saldanha, E., Ratnu, V.S., Priya, R., Adnan, M., Naik, T. S., 2017. Rose Apple (*Syzygium jambos* (L.) Alston), in: Fruit and Vegetable Phytochemicals, pp. 1235–1242.

Bonfanti, G., Bitencourt, P.R., De Bona, K.S., Da Silva, P.S., Jantsch, L.B., Pigatto, A.S., Boligon, A., Athayde, M.L., Gonçalves, T.L., Moretto, M.B., 2013. *Syzygium jambos* and *Solanum guaraniticum* show similar antioxidant properties but induce different enzymatic activities in the brain of rats. Molecules 18 (8), 9179–9194.

Cheng, D.L., Cao, X.P., 1992. Pomolic acid derivatives from the root of *Sanguisorba officinalis*. Phytochemistry 31 (4), 1317–1320.

Dhanabalan, R., Palaniswamy, M., Devakumar, J., 2014. *In vivo* antiplasmodial activity of four folklore medicinal plants used among tribal communities of Western Ghats, Coimbatore, Tamil Nadu. J. Pharm. Res. 8 (6), 751–759.

Díaz-de-Cerio, E., Gómez-Caravaca, A.M., Verardo, V., Fernández-Gutiérrez, A., Segura-Carretero, A., 2016. Determination of guava (*Psidium guajava* L.) leaf phenolic compounds using HPLC-DAD-QTOF-MS. J. Funct. Foods 22, 376–388.

Do, Q.D., Angkawijaya, A.E., Tran-Nguyen, P.L., Huynh, L.H., Soetaredjo, F.E., Ismadji, S., Ju, Y.H., 2014. Effect of extraction solvent on total phenol content, total flavonoid content, and antioxidant activity of *Limnophila aromatica*. J. Food Drug Anal. 22 (3), 296–302.

Eriksson, L., Byrne, T., Johansson, E., Trygg, J., Vikstrom, C., 2006. Process Analytical Technology (PAT) and Quality by Design (QbD), in: Multi- and Megavariate Data Analysis: Basic Principles and Applications, pp. 323–355.

Gavillán-suárez, J., Aguilar-perez, A., Rivera-ortiz, N., Rodríguez-tirado, K., Figueroa-cuilan, W., Morales-santiago, L., Maldonado-martínez, G., Cubano, L.A., Martínez-montemayor, M.M., 2015. Chemical profile and *in vivo* hypoglycemic effects of *Syzygium jambos*, *Costus speciosus* and *Tapeinochilos ananassae* plant extracts used as diabetes adjuvants in Puerto Rico. BMC Complem. Altern. m. 15 (244), 1–15.

Gorst-Allman, C.P., Spiteller, G., 1988. Investigation of lipoxygenase-like activity in strawberry homogenates. Z. Lebensm. Unters. Forsch. 187 (4), 330–333.

Grace, M.H., Warlick, C.W., Neff, S.A., Lila, M.A., 2014. Efficient preparative isolation and identification of walnut bioactive components using high-speed counter-current chromatography and LC-ESI-IT-TOF-MS. Food Chem. 158, 229–238.

Guo, S., Duan, J.ao, Tang, Y., Qian, Y., Zhao, J., Qian, D., Su, S., Shang, E., 2011. Simultaneous qualitative and quantitative analysis of triterpenic acids, saponins and flavonoids in the leaves of two *Ziziphus* species by HPLC-PDA-MS/ELSD. J. Pharmaceut. Biomed. 56(2), 264–270.

Hossain, H., Rahman, S.E., Akbar, P.N., Khan, T.A., Rahman, M.M., Jahan, I.A., 2016. HPLC profiling, antioxidant and *in vivo* anti-inflammatory activity of the ethanol extract of *Syzygium jambos* available in Bangladesh. BMC Res. Notes 9 (191), 1–8.

Hsu, F.F., Turk, J., Williams, T.D., Welti, R., 2007. Electrospray ionization multiple stage quadrupole ion-trap and tandem quadrupole mass spectrometric studies on phosphatidylglycerol from *Arabidopsis* leaves. J. Am. Soc. Mass Spectr. 18 (4), 783–790.

Islam, R., Parvin, M.S., Islam, E., 2012. Antioxidant and hepatoprotective activity of an ethanol extract of *Syzygium jambos* (L.) leaves. Drug Discov. Ther. 6 (4), 205–211.

Jayasinghe, U.L.B., Ratnayake, R.M.S., Medawala, M.M.W.S., Fujimoto, Y., 2007. Dihydrochalcones with radical scavenging properties from the leaves of *Syzygium jambos*. Nat. Prod. Res. 21 (6), 551–554.

Khoo, L.W., Mediani, A., Zolkeflee, N.K.Z., Leong, S.W., Ismail, I.S., Khatib, A., Shaari, K., Abas, F., 2015. Phytochemical diversity of *Clinacanthus nutans* extracts and their bioactivity correlations elucidated by NMR based metabolomics. Phytochem. Lett. 14, 123–133.

Kim, H.K., Choi, Y.H., Verpoorte, R., 2011. NMR-based plant metabolomics: Where do we stand, where do we go? Trends Biotechnol. 29 (6), 267–275.

Kubica, P., Kot-Wasik, A., Wasik, A., Namieśnik, J., Landowski, P., 2012. Modern approach for determination of lactulose, mannitol and sucrose in human urine using HPLC-MS/MS for the studies of intestinal and upper digestive tract permeability. J. Chromatogr. B 907, 34–40.

Kumar, S., Pandey, A.K., 2013. Chemistry and biological activities of flavonoids: An overview. Sci. World J. 1–16.

Kumar, K., Srivastav, S., Sharanagat, V.S., 2021. Ultrasound assisted extraction (UAE) of bioactive compounds from fruit and vegetable processing by-products: A review. Ultrason. Sonochem. 70, 105325.

Lantzouraki, D.Z., Sinanoglou, V.J., Tsiaka, T., Proestos, C., Zoumpoulakis, P., 2015. Total phenolic content, antioxidant capacity and phytochemical profiling of grape and pomegranate wines. RSC Adv. 5, 101683–101692.

Lee, S.Y., Mediani, A., Ismail, I.S., Maulidiani, Abas, F., 2019. Antioxidants and α-glucosidase inhibitors from *Neptunia oleracea* fractions using $^1$H NMR-based metabolomics approach and UHPLC-MS/MS analysis. BMC Complem. Altern. M. 19 (1), 1–15.

Lobo, V., Patil, A., Phatak, A., Chandra, N., 2010. Free radicals, antioxidants and functional foods: Impact on human health. Phcog. Rev. 4 (8), 118–126.
Mahmoud, M.F., Abdelaal, S., Mohammed, H.O., El-Shazly, A.M., Daoud, R., El Raey, M. A., Sobeh, M., 2021. *Syzygium jambos* extract mitigates pancreatic oxidative stress, inflammation and apoptosis and modulates hepatic IRS-2/AKT/GLUT4 signaling pathway in streptozotocin-induced diabetic rats. Biomed. Pharmacother. 142, 112085.
Manguro, L.O.A., Owuor, P.O., Ochung, A.A., 2018. Isolation, characterization and biological activities of phytoconstituents from *Lonchocarpus eriocalyx* Harms leaves. Trends Phytochem. Res. 2 (3), 135–146.
Mediani, A., Abas, F., Tan, C.P., Khatib, A., 2014. Effects of different drying methods and storage time on free radical scavenging activity and total phenolic content of *Cosmos caudatus*. Antioxidants 3 (2), 358–370.
Miller, G.L., 1959. Use of dinitrosalicylic acid reagent for determination of reducing sugar. Anal. Chem. 31 (3), 426–428.
Minkler, P.E., Hoppel, C.L., 2010. Separation and characterization of cardiolipin molecular species by reverse-phase ion pair high-performance liquid chromatography-mass spectrometry. J. Lipid Res. 51 (4), 856–865.
Morton, J., 1987. Rose Apple, in: Fruits of warm climates, pp. 383–386.
Muchembled, J., Sahraoui, A.L.H., Laruelle, F., Palhol, F., Couturier, D., Grandmougin-Ferjani, A., Sancholle, M., 2005. Methoxylated fatty acids in *Blumeria graminis* conidia. Phytochem. 66 (7), 793–796.
Ochieng, M.A., Bakrim, W.B., Bitchagno, G.T.M., Mahmoud, M.M., Sobeh, M., 2022. *Syzygium jambos* L. Alston: An insight into its phytochemistry, traditional uses, and pharmacological properties. Front. Pharmacol. 13, 1–16.
Olsen, J.V., de Godoy, L.M., Li, G., Macek, B., Mortensen, P., Pesch, R., Makarov, A., Lange, O., Horning, S., Mann, M., 2005. Parts per million mass accuracy on an Orbitrap mass spectrometer via lock mass injection into a C-trap. Mol. Cell. Proteomics 4 (12), 2010–2021.
Park, Y.J., Kim, W.S., Ko, S.H., Lim, D.S., Lee, H.J., Lee, W.Y., Lee, D.W., 2003. Separation and characterization of chlorophyll degradation products in silkworm using HPLC-UV-APCI-MS. J. Liq. Chromatogr. R. T. 26 (19), 3183–3197.
Pereira, G.A., Arruda, H.S., Morais, D.R., Eberlin, M.N., Pastore, G.M., 2018. Carbohydrates, volatile and phenolic compounds composition, and antioxidant activity of calabura (*Muntingia calabura* L.) fruit. Food Res. Int. 108, 264–273.
Plaza, M., Batista, Â.G., Cazarin, C.B.B., Sandahl, M., Turner, C., Östman, E., Maróstica Júnior, M.R., 2016. Characterization of antioxidant polyphenols from *Myrciaria jaboticaba* peel and their effects on glucose metabolism and antioxidant status: A pilot clinical study. Food Chem. 211, 185–197.
Pramai, P., Abdul Hamid, N.A., Mediani, A., Maulidiani, M., Abas, F., Jiamyangyuen, S., 2018. Metabolite profiling, antioxidant, and α-glucosidase inhibitory activities of germinated rice: nuclear-magnetic-resonance-based metabolomics study. J. Food Drug Anal. 26 (1), 47–57.
Puech, J.L., Mertz, C., Michon, V., Le Guernevé, C., Doco, T., Hervé Du Penhoat, C., 1999. Evolution of castalagin and vescalagin in ethanol solutions. Identification of new derivatives. J. Agr. Food Chem. 47(5), 2060–2066.
Regueiro, J., Sánchez-González, C., Vallverdú-Queralt, A., Simal-Gándara, J., Lamuela-Raventós, R., Izquierdo-Pulido, M., 2014. Comprehensive identification of walnut polyphenols by liquid chromatography coupled to linear ion trap-orbitrap mass spectrometry. Food Chem. 152, 340–348.
Rice-Evans, C.A., Miller, N.J., Paganga, G., 1996. Structure-antioxidant activity relationships of flavonoids and phenolic acids. Free Radic. Bio. Med. 20 (7), 933–956.
Savić, I.M., Nikolić, V.D., Savić, I.M., Nikolić, L.B., Jović, M.D., Jović, M.D., 2014. The qualitative analysis of the green tea extract using ESI-MS method. Adv. Technol. 3 (1), 30–37.
Sharma, R., Kishore, N., Hussein, A., Lall, N., 2013. Antibacterial and anti-inflammatory effects of *Syzygium jambos* L. (Alston) and isolated compounds on acne vulgaris. BMC Complem. Altern. M. 13 (292), 1–10.
Slatnar, A., Mikulic-Petkovsek, M., Stampar, F., Veberic, R., Solar, A., 2015. Identification and quantification of phenolic compounds in kernels, oil and bagasse pellets of common walnut (*Juglans regia* L.). Food Res. Int. 67, 255–263.
Sobeh, M., Esmat, A., Petruk, G., Abdelfattah, M.A.O., Dmirieh, M., Monti, D.M., Abdel-Naim, A.B., Wink, M., 2018. Phenolic compounds from *Syzygium jambos* (Myrtaceae) exhibit distinct antioxidant and hepatoprotective activities *in vivo*. J. Funct. Foods 41, 223–231.
Song, M., Hang, T.J., Wang, Y., Jiang, L., Wu, X.L., Zhang, Z., Shen, J., Zhang, Y., 2006. Determination of oleanolic acid in human plasma and study of its pharmacokinetics in Chinese healthy male volunteers by HPLC tandem mass spectrometry. J. Pharmaceut. Biomed. 40 (1), 190–196.
Sumanont, Y., Murakami, Y., Tohda, M., Vajragupta, O., Matsumoto, K., Watanabe, H., 2004. Evaluation of the nitric oxide radical scavenging activity of manganese complexes of curcumin and its derivative. Biol. Pharm. Bull. 27 (2), 170–173.
Sun, H., Saeedi, P., Karuranga, S., Pinkepank, M., Ogurtsova, K., Duncan, B.B., Stein, C., Basit, A., Chan, J.C.N., Mbanya, J.C., Pavkov, M.E., Ramachandaran, A., Wild, S.H., James, S., Herman, W.H., Zhang, P., Bommer, C., Kuo, S., Boyko, E.J., Magliano, D. J., 2022. IDF Diabetes Atlas: Global, regional and country-level diabetes prevalence estimates for 2021 and projections for 2045. Diabetes Res. Clin. Pr. 183, 109119.
Taamalli, A., Iswaldi, I., Arráez-Román, D., Segura-Carretero, A., Fernández-Gutiérrez, A., Zarrouk, M., 2013. UPLC-QTOF/MS for a rapid characterisation of phenolic compounds from leaves of *Myrtus communis* L. Phytochem. Anal. 25 (1), 89–96.
Telagari, M., Hullatti, K., 2015. *In-vitro* α-amylase and α-glucosidase inhibitory activity of *Adiantum caudatum* Linn. and *Celosia argentea* Linn. extracts and fractions. Indian J. Pharmacol. 47 (4), 425–429.
Tsai, P., Tsai, T., Yu, C., Ho, S., 2007. Comparison of NO-scavenging and NO-suppressing activities of different herbal teas with those of green tea. Food Chem. 103, 181–187.
Valverde Malaver, C.L., Colmenares Dulcey, A.J., Rial, C., Varela, R.M., Molinillo, J.M. G., Macías, F.A., Isaza Martínez, J.H., 2019. Hydrolysable tannins and biological activities of *Meriania hernandoi* and *Meriania nobilis* (Melastomataceae). Molecules 24 (4), 746–761.
Wan, C., Yuan, T., Cirello, A.L., Seeram, N.P., 2012. Antioxidant and α-glucosidase inhibitory phenolics isolated from highbush blueberry flowers. Food Chem. 135 (3), 1929–1937.
Wolfender, J., Rudaz, S., Choi, Y.H., Kim, H.K., 2013. Plant metabolomics: From holistic data to relevant biomarkers. Curr. Med. Chem. 20, 1056–1090.
Wong, P.L., Fauzi, N.A., Mohamed Yunus, S.N., Abdul Hamid, N.A., Zolkeflee, N.K.Z., Abas, F., 2020. Biological activities of selected plants and detection of bioactive compounds from *Ardisia elliptica* using UHPLC-Q-Exactive Orbitrap mass spectrometry. Molecules 25 (13), 3067–3082.
World Health Organization (WHO), 2016. Global report on diabetes, pp 1-83.
Xia, B., Bai, L., Li, X., Xiong, J., Xu, P., Xue, M., 2015. Structural analysis of metabolites of asiatic acid and its analogue madecassic acid in zebrafish using LC/IT-MS. Molecules 20 (2), 3001–3019.
Yang, L.L., Lee, C.Y., Yen, K.Y., 2000. Induction of apoptosis by hydrolyzable tannins from *Eugenia jambos* L. on human leukemia cells. Cancer Lett. 157, 65–75.
Zhang, Q., Zhang, J., Shen, J., Silva, A., Dennis, D.A., Barrow, C.J., 2006. A simple 96-well microplate method for estimation of total polyphenol content in seaweeds. J. Appl. Phycol. 18 (3–5), 445–450.